arXiv:1406.1991v1 [math.NA] 8 Jun 2014

An Iterative Minimization Formulation for Saddle-Point Search

Weiguo Gao*[1,2], Jing Leng[1], Xiang Zhou†[3]

[1]School of Mathematical Sciences, Fudan University, Shanghai, 200433, China.
[2]MOE Key Laboratory of Computational Physical Sciences, Fudan University, Shanghai, 200433, China.
[3]Department of Mathematics, City University of Hong Kong, Tat Chee Ave, Kowloon, Hong Kong.

June 10, 2014

Abstract

This paper proposes and analyzes an iterative minimization formulation for searching index-1 saddle points of an energy function. This formulation differs from other eigenvector-following methods by constructing a new objective function near the guess at each iteration step. This leads to a quadratic convergence rate, in comparison to the linear case of the gentlest ascent dynamics (E and Zhou, nonlinearity, vol 24, p1831, 2011) and many other existing methods. We also propose the generalization of the new methodology for saddle points of higher index and for constrained energy functions on manifold.

Keywords: saddle point, energy landscape, eigenvector-following, gentlest ascent dynamics, iterative minimization

Mathematics Subject Classification (2010) Primary 65K05, Secondary 82B05

1. Introduction

There have been considerable attentions for a long time to numerical methods of searching local minima of a continuous nonlinear function. The widespread availability of the efficient optimization algorithms for large scale problems has greatly assisted the numerical studies of theoretical physics, chemistry and biology. In computational chemistry, for example, it is of great interest to look for metastable states of molecular configurations, which correspond to local minima of an energy function. Normally, the traditional optimization procedures are very successful at locating a nearby metastable state. However, of more interest is the transition states in these molecular systems, which are the saddle points of the energy function. When it comes to the location of the transitions states, the minimization approach leaves a lot to be desired.

Transition states are characterized as stationary points having one, and only one, negative Hessian eigenvalues (e.g. see [25]). This type of saddle points is usually named

*email: *wggao@fudan.edu.cn.*
†email: *xiang.zhou@cityu.edu.hk.* Corresponding address: Department of mathematics, City University of Hong Kong, Tat Chee Ave, Kowloon, Hong Kong SAR.

as the index-1 saddle points. There have already been a various number of advanced algorithms during the past decades and have proved more efficiently in searching saddles for many practical problems in chemistry and material sciences. The contributions include, but not limited to, the following list: the activation-relaxation techniques[20], the dimer method [13], the nudged elastic band method[15], and the string method[9, 10, 23]. Interested readers can refer to the reference [12]. The first two methods in the above list are the examples of "single-state" (or "surface walker") algorithms and the last two are examples of "chain-of-state" algorithms. The "single-state" algorithms mainly follow the "eigenvector-following" methodology [7, 6, 25] — the system is moved uphill along the eigenvector ("min-mode") corresponding to the smallest eigenvalue of the Hessian matrix . Therefore, these methods drive the system away from the local minimum and push it to some index-1 saddle point if the convergence is achieved. Numerous applications to practical problems have shown that these "eigenvector-following" -type (or "min-mode") methods generally have a much larger attraction domain for convergence to index-1 saddle points than the root-finding methods. In addition, the specificity of selecting index-1 saddles renders these methods more favorable than the root-finding methods. One more benefit of using "eigenvector-following" ideas over the Newton's root-finding method is that the explicit information of Hessian matrix is usually not required in numerical implementation.

Recently, there are rising mathematical interests in writing the "eigenvector-following" methodology [7] in the form of a dynamical system. For instance, one of the authors have proposed the "gentlest ascent dynamics" (GAD)[11, 24], which is a coupled dynamical system of both a position variable and a direction variable. A different but similar dynamical system for the dimer method[13] is further pursued in [27] by introducing one more dimer length variable.

In GAD, the dynamics flow is defined on the product space of the position in the configuration space and the direction in its tangent space. The position variable describes the escape trajectory from the basins of attraction of the local minima. The direction variable in GAD simultaneously evolves to try to follow the min-mode of the Hessian matrix, although it does not have to be exactly the min-mode at any time. It is proved that the stable equilibrium points of this dynamical system are the index-1 saddle points of the energy function while the local minima of the energy function are turned into the index-1 saddle points of GAD. This interesting property invites one to attempt to think of GAD as a counterpart of the very basic steepest descent dynamics (SDD), which converges to a local minimum as time goes to infinity. GAD and SDD are both the simplest flow based on the gradient of the energy function in the configuration space and the convergence rates are both linear for these two methods.

SDD is closely related the steepest descent method, the simplest gradient method for unconstrained optimization, which can be traced back to Cauchy [5]. The analogy between SDD and GAD is a tentative attempt to compare the framework of various optimization algorithms and that of the saddle search algorithms. It is well known that the steepest descent method is ineffective for unconstrained optimization because of its slow convergence rate. Historically, many better alternative optimization techniques have been developed to achieve superlinear or quadratic convergence rate, for instance, Newton's method, L-BFGS, nonlinear conjugate gradient method, and so on [21]. We

are interested to ask what could be the possible analogues of these advanced optimization methods in the context of saddle search problem and how to improve the linear convergence of the GAD as well as other popular saddle search algorithms.

Our motivation is thus to follow the above mentality and includes the following two-fold tasks. Firstly, we want to present a new mathematical framework with connection to some optimization problem, rather than in form of a dynamical system, with the hope that the GAD is a natural "gradient flow" of the associated optimization problem. Secondly, the new formulation should be able to provide a super linear or quadratic convergence rate and carry more flexibility in designing faster algorithms. This paper focuses on the first goal in theoretical aspect and a partial discussion of the second goal with preliminary numerical experiments. The full discussion of developing faster numerical methods and applying to real problems will be presented in a separate article.

The formulation we propose in this note is an iterative minimization scheme. At each iteration, a new objective function is constructed based on the given energy function by using the information of the current values of the position and the eigenvector of the smallest eigenvalue. Then a local minimizer of this objective function is assigned to the new value of the position at the next iteration. This iterative scheme can be completely described by a continuously differentiable mapping. We discover that the Jacobian matrix of this mapping vanishes at the saddle point and it follows that the convergence rate of the iterative minimization scheme is quadratic.

The authors notice that a few variant techniques have been proposed in efforts to improve the efficiency of the "single-state"-type algorithms for saddle search, such as [14, 16, 4, 17]. However, all these methods either improve the rotation step of solving the eigenvector or improve the translation step of moving the position in *the* dimension along the obtained direction. The resulting overall effect on the errors actually still only has the linear convergence rate in the configuration space.

The rest of this paper is organized as follows. We first briefly review the gentlest ascent dynamics in Section 2. In Section 3, we formulate our iterative minimization scheme for index-1 saddles and analyze the convergence rate. We also discuss the situation with constraints for saddle points in Section 4. The generalization for index-m ($m > 1$) saddles are discussed in Section 5. Several numerical examples are presented in Section 6 to illustrate our theory. Section 7 is the concluding remarks.

2. Review of gentlest ascent dynamics (GAD)

The gentlest ascent dynamics is a mathematical model in form of the dynamical system to describe the escape of the basin of attractions in the gentlest way and the convergence to a saddle. Given a smooth energy function V on the configuration space, say $\mathbb{R}^d$, the gentlest ascent dynamics is the following dynamic system defined on the phase space $\mathbb{R}^d \times \mathbb{R}^d$

$$\begin{cases} \dot{x} = -\nabla V(x) + 2\dfrac{\langle \nabla V(x), v\rangle}{\langle v, v\rangle} v, & \text{(1a)} \\ \gamma \dot{v} = -\nabla^2 V(x) v + \dfrac{\left\langle v, \nabla^2 V(x) v\right\rangle}{\langle v, v\rangle} v. & \text{(1b)} \end{cases}$$

Here $\langle \cdot, \cdot \rangle$ is the dot product in the Euclidean space $\mathbb{R}^d$ and the relaxation constant γ can be any positive real number. The second equation (1b) attempts to find the direction that corresponds to the smallest eigenvalue of the Hessian matrix $\nabla^2 V(x)$. The second

term is to impose the normalization condition that $\|v\| = \sqrt{\langle v, v\rangle} = 1$. The last term in the first equation (1a) reverses the component of the gradient force in the direction v to drive the system uphill in the direction of v.

It is shown in [11] that the saddle point of the original function V is the stable equilibrium point of the GAD. We recall this result in the following proposition for convenience.

Proposition. Assume that the energy function V is $\mathcal{C}^4(\mathbb{R}^d;\mathbb{R})$.

(a) If (x_*, v_*) is an equilibrium point of the gentlest ascent dynamics (1) and $\|v_*\| = 1$, then v_* is an eigenvector of $\nabla^2 V(x_*)$ corresponding to one eigenvalue λ_*, and x_* is an equilibrium point of the steepest descent dynamics of V, i.e., $\nabla V(x_*) = 0$.

(b) Suppose that x_s is a stationary point of V, i.e., $\nabla V(x_s) = 0$. Let $v_1, v_2, \cdots, v_d$ be the normalized eigenvectors of the Hessian $\nabla^2 V(x_s)$, and the associated eigenvalues be $\lambda_1, \lambda_2, \cdots, \lambda_d$, respectively. Then for all $i = 1, \cdots, d$, (x_s, v_i) is an equilibrium point of the gentlest ascent dynamics (1). Furthermore, among these d equilibrium points, there exists one pair $(x_s, v_{i'})$ which is linearly stable for gentlest ascent dynamics (1), if and only if x_s is an index-1 saddle point of the function V, or equivalently, the eigenvalue $\lambda_{i'}$ corresponding to $v_{i'}$ is the only negative eigenvalue of $\nabla^2 V(x_s)$.

When the GAD converges, v corresponds to the smallest eigenvalue of the Hessian $H(x) \triangleq \nabla^2 V(x)$ at the saddle point x_s. Actually, for any frozen x in the equation (1b), the steady state of the solution $v(t)$ solves the following minimization problem for Rayleigh quotient

$$\min_{\|u\|=1} u^{\mathsf{T}} H(x) u, \tag{2}$$

and the equation (1b) is just a steepest descent dynamics (rescaled in time by γ) for the minimization problem (2). In the limit of $\gamma \to 0$, $v(t)$ approaches the eigenvector of the smallest eigenvalue instantly, and GAD is reduced to traditional "eigenvector-following" methodology. In this case, v can be viewed as a function $v(x)$. For finite γ, the equation (1) couples the dynamics of x and v simultaneously and still preserves the convergence to saddle points.

In contrast to the flow for v, the dynamics equation (1a) for the position x, however, is *not* in the form of the steepest descent dynamics of some scalar function. To see this, denoting the GAD force as $F(x)$:

$$F_i(x) \triangleq f_i(x) - 2\sum_k v_i f_k(x) v_k$$

where $f(x) \triangleq -\nabla V(x)$. It is easy to see that $\frac{\partial F_i}{\partial x_j} = -H_{ij} + 2v_i \sum_k H_{kj} v_k = -H + 2vv^{\mathsf{T}} H$ while its transpose $\frac{\partial F_j}{\partial x_i} = -H + 2Hvv^{\mathsf{T}}$. The necessary condition for the dynamics of x being of a gradient type is that the Hessian H commutes with the rank-1 matrix vv^{T}, which generally does not hold since v may not be the exact eigenvector of H in GAD. Even in the $\gamma \to 0$ limit where $v = v(x)$ is indeed the eigenvector of $H(x)$, the Jacobian matrix for $F_i(x) = f_i(x) - 2\sum_k v_i(x) f_k(x) v_k(x)$ is still not symmetric.

Therefore, the GAD is not as simple as a steepest descent flow and no underlying energy function to drive this dynamics. In the next section, we shall show that the GAD can be approximated by a steepest descent flow of a new objective function which is locally constructed. This leads to an iterative minimization formulation.

3. The Iterative minimization formulation

In this section, we discuss how to define a new objective function to drive the system toward an index-1 saddle point of the original energy function. The intuitive idea is to change the sign of the energy function V along some direction, rather than reversing the direction of the force as in the GAD. The resulting Hessian then changes the sign of the smallest eigenvalue while keeps the other eigenvalues the same.

3.1. **The iterative scheme.** The framework we start with is the following iterative expression

$$\begin{cases} v^{(k+1)} = \underset{\|u\|=1}{\operatorname{argmin}}\ u^{\mathsf{T}} H(x^{(k)}) u, & \text{(3a)} \\ x^{(k+1)} = \underset{y}{\operatorname{argmin}}\ \left(V(y) + W^{(k)}(y) \right), & \text{(3b)} \end{cases}$$

where $W^{(k)}$ is an unknown function to be determined. We need construct $W^{(k)}$ such that $x^{(k)}$ converges to a saddle point of V.

The following two choices of the function $W^{(k)}$ serve our purpose.

$$W_1^{(k)}(y) = W_1(y; x^{(k)}, v^{(k+1)}), \qquad W_2^{(k)}(y) = W_2(y; x^{(k)}, v^{(k+1)}), \tag{4}$$

where with the abuse of the notation, we define

$$W_1(y; x, v) \triangleq -2V(y) + 2V\left(y - vv^{\mathsf{T}}(y - x) \right), \tag{5}$$

$$W_2(y; x, v) \triangleq -2V\left(x + vv^{\mathsf{T}}(y - x) \right). \tag{6}$$

which are two $\mathbb{R}^d \to \mathbb{R}$ functions parameterized by the position x and the normalized direction v. Therefore, the new objective function $V+W$ depends on the current position x and the direction v. In equation (4) for the choice of $W^{(k)}$, the direction $v^{(k+1)}$ is computed from the given $x^{(k)}$ via the Hessian matrix. Therefore, the equation (3) is actually an iterative scheme mapping $x^{(k)}$ to $x^{(k+1)}$.

Given a position x and a direction v, we then have an affine hyperplane, denoting as $\mathcal{P}_{x,v}$, through x with the normal v, i.e., $\mathcal{P}_{x,v} = \{y : (y - x)^{\mathsf{T}} v = 0\}$. Introduce the projection matrix Π_v and $\Pi_v^{\perp} = \mathrm{I} - \Pi_v$, where

$$\Pi_v u = vv^{\mathsf{T}} u.$$

Then, the argument in the second term of W_1 is the point

$$y - vv^{\mathsf{T}}(y - x) = x + \Pi_v^{\perp}(y - x),$$

which is the projection of the point y on the affine hyperplane $\mathcal{P}_{x,v}$. The position in W_2, $x + vv^{\mathsf{T}}(y - x) = x + \Pi_v(y - x)$, is the projection on the ray at x with the direction v.

The intuition of the definitions of W_1 and W_2 is the following. If y lies on the ray along v, then $W_2 = -2V(y)$. Consequently, the new energy function $V(y) + W_2(y; x, v)$ is to modify the potential $V(y)$ by reversing the sign of V in the direction v. For the choice of $V(y) + W_1(y; x, v)$, which is equal to $-V(y) + 2V(x + \Pi^{\perp}(y - x))$, can viewed as the reverse of the sign of $-V$ (instead of V) on the $d-1$ dimensional affine plane $\mathcal{P}_{x,v}$. Let us take a simple example of the quadratic function $V(y) = \frac{1}{2}\sum_{i=1}^{d} \mu_i y_i^2$

where $\mu_1 < 0 < \mu_2 < \cdots < \mu_d$. The zero vector is the index-1 saddle point of V. $v = (1, 0, \cdots, 0)$ is the eigenvector corresponding to the smallest eigenvalue μ_1. Then,

$$V(y) + W_1(y; x, v) = \mu_1 x_1^2 - \frac{1}{2}\mu_1 y_1^2 + \frac{1}{2}\sum_{i=2}^{d} \mu_i y_i^2,$$

$$V(y) + W_2(y; x, v) = -\sum_{i=2}^{d} \mu_i x_i^2 - \frac{1}{2}\mu_1 y_1^2 + \frac{1}{2}\sum_{i=2}^{d} \mu_i y_i^2.$$

The difference of the above two functions of y is just a constant $2V(x)$. Both of them are the convex quadratic functions of y and they share the same Hessian matrix $\mathrm{diag}\{-\mu_1, \mu_2, \cdots, \mu_d\}$ and the same minimizer 0, which is exactly the saddle point of V. So for any initial position $x^{(0)}$, the next iteration $x^{(1)}$ is the true solution.

3.2. **Convergence result.** We have formulated the saddle search problem as a fixed point problem in the iterative scheme (3) together with the defined W_1 and W_2 in (5) and (6). In fact, the function $W^{(k)}$ in the iterative scheme (3) can be some linear combination of W_1 and W_2 to achieve our purpose, too. In addition, the constant 2 showing in W_1 and W_2 can be relaxed. In the next, we shall consider this general case to define the mapping from $x^{(k)}$ to $x^{(k+1)}$. Denote this mapping for the iteration as $\Phi(x)$. We shall show that the Jacobian matrix of Φ vanishes at the index-1 saddle point. This implies the iterative scheme is of quadratic convergence.

Theorem 1. *Assume that $V(x) \in \mathcal{C}^3(\mathbb{R}^d; \mathbb{R})$. For each x, let $v(x)$ be the normalized eigenvector corresponding to the smallest eigenvalue of the Hessian matrix $H(x) = \nabla^2 V(x)$, i.e.,*

$$v(x) = \underset{u \in \mathbb{R}^d,\, \|u\|=1}{\operatorname{argmin}} \; u^T H(x) u.$$

Given two real numbers α and β satisfying $\alpha + \beta > 1$, we define the following function of the variable y,

$$\begin{aligned} L(y; x, \alpha, \beta) = (1-\alpha)V(y) + \alpha V\Big(y - v(x)v(x)^T(y-x)\Big) \\ -\beta V\Big(x + v(x)v(x)^T(y-x)\Big). \end{aligned} \tag{7}$$

Suppose that x^* is an index-1 saddle point of the function $V(x)$, i.e, $\nabla V(x^*)$ has only one negative eigenvalue $\lambda(x^*)$. Then the following statements are true.

- *(i) x^* is a local minimizer of $L(y; x^*, \alpha, \beta)$.*
- *(ii) There exists a neighborhood $\mathcal{U}$ of x^* such that for any $x \in \mathcal{U}$, $L(y; x, \alpha, \beta)$ is strictly convex in $y \in \mathcal{U}$ and thus has a unique minimum in $\mathcal{U}$.*
- *(iii) Define the mapping $\Phi : x \in \mathcal{U} \to \Phi(x) \in \mathcal{U}$ to be the unique local minimizer of L in $\mathcal{U}$ for any $x \in \mathcal{U}$. Further assume that $\mathcal{U}$ contains no other stationary point of V except x^*. Then the mapping Φ has only one fixed point x^* .*
- *(iv) $\Phi(x)$ is differentiable in $\mathcal{U}$. The derivative of Φ vanishes at x^*, i.e., the Jacobi matrix*

$$\Phi_x(x^*) = 0. \tag{8}$$

Proof. Part (i):

We calculate the first and second derivative of $L(y;x,\alpha,\beta)$ with respect to y. The first order derivative is

$$\begin{aligned}\nabla_y L = (1-\alpha)\nabla V(y) + \alpha(I - vv^{\mathsf{T}})\nabla V\left(y - vv^{\mathsf{T}}(y-x)\right)\\ -\beta vv^{\mathsf{T}}\nabla V\left(x + vv^{\mathsf{T}}(y-x)\right).\end{aligned} \tag{9}$$

So, it is clear that $\nabla_y L(x^*;x^*,\alpha,\beta) = 0$ for any constants α and β since $\nabla V(x^*) = 0$.

The Hessian matrix of L is

$$\begin{aligned}\nabla_y^2 L(y;x,\alpha,\beta) =&(1-\alpha)\nabla^2 V(y) + \alpha(I - vv^{\mathsf{T}})\nabla^2 V(y - vv^{\mathsf{T}}(y-x))(I - vv^{\mathsf{T}})\\ &- \beta vv^{\mathsf{T}}\nabla^2 V(x + vv^{\mathsf{T}}(y-x))vv^{\mathsf{T}},\end{aligned} \tag{10}$$

which is simplified at $y = x^*$ and $x = x^*$ as follows

$$\nabla_y^2 L(x^*;x^*,\alpha,\beta) = H(x^*) - (\alpha+\beta)\lambda(x^*)v(x^*)v(x^*)^{\mathsf{T}}.$$

where the fact $H(x^*)v(x^*) = \lambda(x^*)v(x^*)$ is applied. Since $\lambda(x^*) < 0$, then $\nabla_y^2 L(x^*;x^*,\alpha,\beta)$ is positive definite if $\alpha + \beta > 1$.

Part (ii)

The assumption that $V \in \mathcal{C}^3$ and x^* is the index-1 saddle of V implies that the eigendirection $v(x)$ is continuously differentiable at x^*. Then Equation (10), together with the continuity of $\nabla^2 V(x)$ and $v(x)$ at x^*, implies that the Hessian, $\nabla_y^2 L(y;x,v(x))$, which is treated now as a function of two variables y and x, is continuously differentiable at $(y,x) = (x^*,x^*)$. In *Part (i)*, we proved that at the point (x^*,x^*), the Hessian is positive-definite as $\alpha+\beta > 1$. Thus, there exists a neighborhood of (x^*,x^*), denoted as $\mathcal{N}$, such that the Hessian $\nabla_y^2 L(y;x)$ at each $(y,x) \in \mathcal{N}$ is still positive-definite. Select a neighorhood in the form of product of two convex sets $\mathcal{U}\times\mathcal{U}$ inside the $2d$-dim set $\mathcal{N}$, then the set $\mathcal{U}$ is the desired one.

Part (iii): Suppose that there is a second fixed point $\hat{x} \in \mathcal{U}$ such that $\Phi(\hat{x}) = \hat{x}$. Then $\nabla_y L(\hat{x};\hat{x}) = 0$. From the equation (9),

$$\nabla_y L(\hat{x};\hat{x}) = \nabla V(\hat{x}) - (\alpha+\beta)v(\hat{x})v(\hat{x})^{\mathsf{T}}\nabla V(\hat{x}) = 0.$$

Since $\alpha+\beta \neq 1$, then $\nabla V(\hat{x}) = 0$. But there is only one stationary point x^* in $\mathcal{U}$, so $\hat{x}$ has to be the point x^*.

Part (iv):

For each $x_0 \in \mathcal{U}$, $(\Phi(x_0), x_0)$ is the solution of the first order equation $\nabla_y L(\Phi(x_0);x_0) = 0$. It is clear that $\nabla_y L(y;x)$ is continuously differentiable at all (y,x) in $\mathcal{U}\times\mathcal{U}$. In addition, $\nabla_y^2 L(y;x)$ is strictly positive-definite from *Part(ii)*, thus non degenerate in $\mathcal{U}\times\mathcal{U}$. Therefore, the Implicit Function Theorem implies that $\Phi(x)$ is Lipschitz continuous and differentiable near x_0.

Next, we calculate the derivative of the mapping Φ, denoted as $\Phi_x(x)$. For each $x \in \mathcal{U}$, $\Phi(x)$ is a solution of the first order equation (9). Thus the following equation holds

$$(1-\alpha)\nabla V(\Phi(x)) + \alpha\left(I - v(x)v(x)^{\mathsf{T}}\right)\nabla V(\varphi_1(x)) - \beta\, v(x)v(x)^{\mathsf{T}}\nabla V(\varphi_2(x)) = 0. \tag{11}$$

where

$$\varphi_1(x) = \Phi(x) - v(x)v(x)^{\mathsf{T}}(\Phi(x) - x), \qquad \varphi_2(x) = x + v(x)v(x)^{\mathsf{T}}(\Phi(x) - x).$$

Now we take the derivative with respect to x on both sides of (11), then

$$\begin{aligned}(1-\alpha)H(\Phi)\Phi_x + \alpha\left(I - vv^{\mathsf{T}}\right)H(\varphi_1)\varphi_{1,x} - \alpha v^{\mathsf{T}}\nabla V(\varphi_1)J - \alpha v\nabla V(\varphi_1)^{\mathsf{T}}J \\ = \beta vv^{\mathsf{T}}H(\varphi_2)\varphi_{2,x} + \beta v^{\mathsf{T}}\nabla V(\varphi_2)J + \beta v\nabla V(\varphi_2)^{\mathsf{T}}J.\end{aligned} \tag{12}$$

where the derivatives $J = \frac{\partial v(x)}{\partial x}$ and $\Phi_x = \frac{\partial \Phi}{\partial x}$ are the Jacobi matrix of $v(x)$ and $\Phi(x)$ respectively. The derivatives $\varphi_{1,x}$, $\varphi_{2,x}$ are defined similarly.

Note that $\Phi(x^*) = x^*$ thus $\varphi_1(x^*) = \varphi_2(x^*) = x^*$. Consequently $\nabla V(\varphi_1)$ and $\nabla V(\varphi_2)$ both vanish at x^* since $\nabla V(x^*) = 0$. Meanwhile, since

$$\begin{aligned}\varphi_{1,x} &= \Phi_x - vv^{\mathsf{T}}(\Phi_x - I) - v^{\mathsf{T}}(\Phi - x)J - v(\Phi - x)^{\mathsf{T}}J, \\ \varphi_{2,x} &= I + vv^{\mathsf{T}}(\Phi_x - I) + v^{\mathsf{T}}(\Phi - x)J + v(\Phi - x)^{\mathsf{T}}J,\end{aligned}$$

then in particular at $x = x^*$, we have

$$\begin{aligned}\varphi_{1,x}(x^*) &= \left(I - v(x^*)v(x^*)^{\mathsf{T}}\right)\Phi_x(x^*) + v(x^*)v(x^*)^{\mathsf{T}}, \\ \varphi_{2,x}(x^*) &= I - v(x^*)v(x^*)^{\mathsf{T}} + v(x)v(x)^{\mathsf{T}}\Phi_x(x^*).\end{aligned}$$

Therefore, by noting $\nabla V(x^*) = 0$ again, the equation (12) at $x = x^*$ becomes

$$\begin{aligned}&(1-\alpha)H(x^*)\Phi_x(x^*) \\ &+ \alpha\left(I - v(x^*)v(x^*)^{\mathsf{T}}\right)H(x^*)\left(I - v(x^*)v(x^*)^{\mathsf{T}}\right)\Phi_x(x^*) \\ &+ \alpha\left(I - v(x^*)v(x^*)^{\mathsf{T}}\right)\nabla^2 V(x^*)v(x^*)v(x^*)^{\mathsf{T}} \\ &- \beta v(x^*)v(x^*)^{\mathsf{T}}H(x^*)\left(I - v(x^*)v(x^*)^{\mathsf{T}}\right) \\ &- \beta v(x^*)v(x^*)^{\mathsf{T}}H(x^*)v(x^*)v(x^*)^{\mathsf{T}}\Phi_x(x^*) \\ &= 0.\end{aligned} \tag{13}$$

As $v(x)$ is the eigenvector of the Hessian $\nabla^2 V(x)$, i.e., $H(x)v(x) = \lambda(x)v(x)$, it is easy to verify that for each x, $\left(I - v(x)v(x)^{\mathsf{T}}\right)\nabla^2 V(x)v(x)v(x)^{\mathsf{T}} = 0$ holds. Thus, any term in (13) without the Jacobi Φ_x vanishes. So, the equation (13) gives the following linear equation

$$\left(H(x^*) - (\alpha+\beta)\lambda(x^*)v(x^*)v(x^*)^{\mathsf{T}}\right)\Phi_x(x^*) = 0 \tag{14}$$

which implies that $\Phi_x(x^*) = 0$ if and only if $\alpha + \beta \neq 1$.

□

The above theorem implies the important property of the proposed iterative minimizing formulation in §3.1 if the energy function V has a higher regularity $\mathcal{C}^4$.

Corollary 2. *Assume that $V(x) \in \mathcal{C}^4(\mathbb{R}^d; \mathbb{R})$. The iterative scheme $x^{(k+1)} = \Phi(x^{(k)})$ has exactly the second order (local) convergence rate.*

Proof. Since V is $\mathcal{C}^4$, then $\nabla_y L$ has the regularity $\mathcal{C}^2$ and in the neighborhood $\mathcal{U}$. It follows that $\Phi(x)$ is continuously differentiable at x^* based on the second order pseudo expansion ([2]) for the first order equation $\nabla_y L = 0$.

Since $\Phi_x(x^*) = 0$, then there is a neighborhood of x^*, such that $\|\Phi_x(x)\|$ is strictly less than one in this neighborhood. Thus, the local convergence comes from the contraction mapping principle.

The second order convergence rate is due to the Jacobi matrix $\Phi_x(x^*)$ vanishes. One can carry out further calculation and exam that the second derivative of $\Phi(x)$ at x^* does not trivially vanish. So, the iteration $x \to \Phi(x)$ locally converges to x^* exactly at quadratic rate. □

For the quadratic example in §3.1, we have the following trivial result.

Corollary 3. *If $V(x) = \frac{1}{2}x^T H x$ where H is a constant symmetric matrix and has only one negative eigenvalue. Suppose that α, β in Theorem 1 satisfy $\alpha + \beta > 1$. Then $\Phi(x) = 0$ for all x.*

We remark that the $\Phi(x)$ is well-defined in a local neighborhood of x^*. In implementations, the local solution of the new objective function $L(y; x^{(k)})$ in (7) is pursued with the initial guess $y_0 = x^{(k)}$. This choice of the initial guess is not only very simple to pick up but also excludes the possibilities of overshooting to other local solutions which are not relevant to the saddle of interest.

3.3. **Solve subproblem of minimization.** The iterative minimization formulation (3) consists of solving a subproblem of minimization at each iteration. Corollary 2 suggests that the quadratic convergence rate is achieved when the subproblem is solved exactly and the correct local minimizer is found. In practice, one may not need to solve the subproblem of the minimization exactly or with high accuracy and the superlinear convergence may be achieved in certain circumstances. Many existing "eigenvector-following" methods like dimer method could be viewed as some special discretisation for the subproblem.

We first present a result about the connection of the gentlest ascent dynamics and the iterative minimization formulation.

Theorem 4. *Assume $x^{(k)}$ is near the index-1 saddle point x^*. Suppose that one solves the subproblem $\min_y L(y; x^{(k)}, \alpha, \beta)$ in Theorem 1 by only one single steep descent method with the step size δt,*

$$x^{(k+1)} = x^{(k)} - \delta t\, \nabla_y L(x^{(k)}; x^{(k)}, \alpha, \beta). \tag{15}$$

Then the sequence $\{x^{(k)}\}$ is the discrete solution of the Euler method with the time step δt for the following version of the gentlest ascent dynamics

$$\dot{x} = -\nabla V(x) + (\alpha + \beta)\Pi_{v(x)} \nabla V(x). \tag{16}$$

Proof. The conclusion is obvious by noting the following and the fact in equation (9),

$$\begin{aligned} x_{k+1} =& x_k - \delta t\, \nabla_y L(x_k; x_k, \alpha, \beta) \\ &= x_k - \delta t\big((1-\alpha)\nabla V(x_k) + \alpha(I - v(x_k)v(x_k)^{\mathsf{T}}\nabla V(x_k)) \\ &\qquad - \beta v(x_k)v(x_k)^{\mathsf{T}}\nabla V(x_k)\big). \end{aligned}$$

□

Remark 1. *If the subproblem for the direction v is also solved by the steepest descent method, then $(x^{(k)}, v^{(k)})$ corresponds to the original version of GAD* (1).

The subproblem at each iteration consists of the minimization for the position and the direction. Some fast algorithms have been developed for solving the smallest eigenvector problem, in particular where the Hessian is not explicit available and the force is calculated from the first principle [17] . The new numerical challenge to implement the iterative minimization formulation efficiently is the minimization of L for the position to get new $x^{(k+1)}$. Of course, one is not limited to use the steepest descent method to solve this subproblem as in Theorem (4). For example, CG can be applied with certain level of tolerance. Details about these accelerating techniques will be postponed in a separate paper.

We now discuss the choice of two parameters α and β in our formulation. Theoretically by Theorem 1, the condition that $\alpha + \beta > 1$ is sufficient for the algorithm to achieve the local quadratic convergence. In practice, a better choice of α and β may help reduce the condition number of the subproblem, which is ratio of the maximum eigenvalue and the smallest eigenvalue of the Hessian $\nabla_y^2 L$. The calculation in the proof of Theorem 1 has shown that at the saddle point x^*, the eigenvalues of $\nabla_y^2 L$ are $(1-\alpha-\beta)\lambda_1, \lambda_2, \lambda_3, \cdots, \lambda_d$ where $\lambda_1 < 0 < \lambda_2 < \cdots < \lambda_d$ are eigenvalues of $\nabla^2 V(x^*)$. Hence, to minimize the condition number of $\nabla_y^2 L$, the optimal choice of α and β needs to satisfy

$$1 + \frac{\lambda_2}{|\lambda_1|} \leq \alpha + \beta \leq 1 + \frac{\lambda_d}{|\lambda_1|},$$

and the resulting optimal condition number is λ_d/λ_2. In practice, a rough estimate of λ_2 may be used to select the parameter $\alpha + \beta$ at each iteration.

When the initial guess of the iterative method is in the convex region of the original energy function, for example, a local minimum, the function L will have no lower bound locally and the minimization subproblem does not have a solution. One can handle this situation using the traditional techniques implemented in many eigenvector-following-type methods. One simple remedy is to only seek the solution within a ball or hypercube with a proper size around the current solution $x^{(k)}$. Such remedies are not necessarily needed when λ_1 is negative.

4. Saddles on manifold

In some applications, the configuration of the system may be subject to one or more constraints, for instance the conservation laws of some physical quantities. Suppose that these constraints specify a Riemann manifold $\mathcal{M}$ embedded in $\mathbb{R}^d$. The index-1 saddle point of the energy function restricted on $\mathcal{M}$ is still the transition state of interest. The calculation of the saddle point on the manifold calls for the attention for the effect of the constraints. In this section, we want to extend the GAD and iterative minimization scheme onto the manifold $\mathcal{M}$. This goal can be easily achieved for GAD by a simple projection procedure, as in [8, 26]. But it requires extra work for the iterative minimization formulation.

We assume that the manifold $\mathcal{M}$ is characterized by p (independently) equality constraints: $c_i(x) = 0$ for $i = 1, 2, \cdots, p$ where c_i are $\mathbb{R}^d \to \mathbb{R}$ smooth functions. To maintain a right mix of abstraction and concreteness, we use the extrinsic variables x in $\mathbb{R}^d$ for $\mathcal{M}$. The tangent space $\mathcal{T}_x$ at each point x of the manifold $\mathcal{M}$ is thus the orthogonal

complement in $\mathbb{R}^d$ to the normal space spanned by the gradients of the p constraints, $span\{\nabla c_i(x), i = 1, 2, \cdots, p\}$. The concepts of the local minimum and the index-1 saddle point of the smooth energy function $V(x)$ can be extended to the manifold case without any difficulty [1]. We skip the rigorous math definitions since they are quite intuitive.

We start with the calculation of the eigenvector v in the tangent space $\mathcal{T}_x$ corresponding to the smallest eigenvalue of the (projected) Hessian matrix of the energy function V. This direction v minimizes the Rayleigh quotient among all possible vectors in $\mathcal{T}_x$:

$$v = \underset{\|u\|=1, u\in\mathcal{T}_x}{\operatorname{argmin}} \; u^{\mathsf{T}}\nabla^2 V(x)u,$$

or equivalently

$$v = \underset{\|u\|=1, u\in\mathbb{R}^d}{\operatorname{argmin}} \left\{ u^{\mathsf{T}}\nabla^2 V(x)u \,\middle|\, \langle \nabla c_i(x), u\rangle = 0, \forall i = 1, 2, \cdots, p \right\}. \tag{17}$$

The steepest descent flow of this constrained minimization problem is

$$\gamma\dot{v} = -\Pi_{\mathcal{T}_x}\left[\nabla^2 V(x)v\right] + \eta v$$

where $\Pi_{\mathcal{T}_x}$ is the orthogonal projection of $\mathbb{R}^d$ to the vector space $\mathcal{T}_x$ and the scalar $\eta = \left\langle \Pi_{\mathcal{T}_x}\left[\nabla^2 V(x)v\right], v\right\rangle$ is to enforce the unit length of v. Many existing fast algorithms for the original rotation step to solve v in $\mathbb{R}^d$ can be readily modified for the constrained problem (17).

Next, we discuss the dynamics or the iterations for the position variable x. For the dynamics of x in GAD, we can simply project the GAD force $(-\mathrm{I} + 2vv^{\mathsf{T}})\nabla V(x)$ onto the tangent space $\mathcal{T}_x$, i.e.,

$$\dot{x} = \Pi_{\mathcal{T}_x}\left[(-\mathrm{I} + 2vv^{\mathsf{T}})\nabla V(x)\right],$$

then the trajectory of GAD stays on the manifold $\mathcal{M}$ all the time. However, for the iterative minimization formulation (3), the need of projection on $\mathcal{M}$ complicates our discussion. Specifically, for a given $x \in \mathcal{M}$ and $v \in \mathcal{T}_x$, one can find a geodesic curve on $\mathcal{M}$ by following the geodesic flow which can be described in terms of these constraints functions $c_i(x)$ [3]. Let $\xi(s)$ ($s \in \mathbb{R}$) be the geodesic curve satisfying $\xi(0) = x$ and $\xi'(0) = v$. For each point $y \in \mathcal{M}$ near x, under some mild condition, we can define the projection of y onto the geodesic ξ as $\xi(s_y)$ where $s_y \triangleq \operatorname{argmin}_s \operatorname{dist}(\xi(s), y)$. Here "dist" is the distance between two points of the manifold $\mathcal{M}$: infimum of the lengths of all continuously differentiable curve on $\mathcal{M}$ joining these two points. The argument of the W_2 function is then the point which has minimal distance on $\mathcal{M}$ to the curve $\xi(s)$, i.e., the "projection" of y to ξ. Therefore, the counterpart of W_2 on $\mathcal{M}$ is

$$W_2(y) = -2V(\xi(s_y)). \tag{18}$$

In principle, the same strategy can be applied for the W_1 function where the minimal distance to the set of geodesic curves whose tangents are in $\mathcal{T}_x$ but orthogonal to v should be pursued .

In a nutshell, the iterative minimization scheme on the manifold $\mathcal{M}$ specified by the p constraints $c_i(x) = 0$ can be written as follows

$$\begin{cases} x^{(k+1)} = \underset{y}{\operatorname{argmin}} \left\{ V(y) + W^{(k)}(y) \,\middle|\, c_i(y) = 0, \forall i = 1, 2, \cdots, p \right\}, & \text{(19a)} \\ v^{(k+1)} = \underset{\|u\|=1, u\in\mathbb{R}^d}{\operatorname{argmin}} \left\{ u^{\mathsf{T}}\nabla^2 V(x^{(k+1)})u \,\middle|\, \left\langle \nabla c_i(x^{(k)}), u \right\rangle = 0, \forall i \right\}, & \text{(19b)} \end{cases}$$

where $W^{(k)}$ (which depends on $x^{(k)}$ and $v^{(k+1)}$) is defined through the above mentioned W_1, W_2 or their linear combination in the same way as in Theorem 1. To illustrate the above idea, the example of the sphere S^2 in $\mathbb{R}^3$ is presented in Section 6.3. The numerical result for a quadratic energy function on this manifold shows that the iterative scheme (19) also has the quadratic convergence rate.

5. Saddle with higher index

The reference [11] of GAD has extended from the index-1 saddle point to saddle points of index-m for $m > 1$ case with the help of dilation technique. Our new iterative minimization formulation proposed above for the index-1 saddle can also be extended to the case of saddles with index more than 1. Suppose that one has found m eigenvectors of the Hessian matrix $\nabla^2 V(x)$, $v_1, v_2, \cdots, v_m$, corresponding the m smallest eigenvalues, respectively. We denote S as the set of all subsets of $\{1, \ldots, m\}$ except the empty set. For every $s \in S$, we have $s = \{i_1, \ldots, i_k\} \subset \{1, \ldots, m\}$ with $1 \le i_1 < \cdots < i_k \le m$ and $k \le m$. The projection onto the plane spanned by k column vectors $\{v_{i_1}, v_{i_2}, \ldots, v_{i_k}\}$ is associated with the following matrix

$$\Pi_s = V_s V_s^{\mathsf{T}} = \begin{bmatrix} v_{i_1} & v_{i_2} & \cdots & v_{i_k} \end{bmatrix} \begin{bmatrix} v_{i_1}^{\mathsf{T}} \\ v_{i_2}^{\mathsf{T}} \\ \vdots \\ v_{i_k}^{\mathsf{T}} \end{bmatrix}.$$

Let $\Pi_s^{\perp} = \mathrm{I} - \Pi_s$. The objective function for the subproblem, which is a generalization to the equation (7), is now given by

$$\begin{aligned} L(y; x, \alpha, \beta) = \left(1 - \sum_{s \in S} \alpha_s\right) V(y) + \sum_{s \in S} \alpha_s V(x + \Pi_s^{\perp}(y - x)) \\ - \sum_{s \in S} \beta_s V(x + \Pi_s (y - x)). \end{aligned} \tag{20}$$

where $\alpha = (\alpha_s)_{s \in S}$ and $\beta = (\beta_s)_{s \in S}$. For example, the function (20) in the index-2 case is

$$\begin{aligned} L(y; x, \alpha, \beta) &= (1 - \alpha_1 - \alpha_2 - \alpha_{1,2}) V(y) \\ &\quad + \alpha_1 V\left(x + \Pi_1^{\perp}(y - x)\right) + \alpha_2 V\left(x + \Pi_2^{\perp}(y - x)\right) + \alpha_{1,2} V\left(x + \Pi_{1,2}^{\perp}(y - x)\right) \\ &\quad - \beta_1 V\left(x + \Pi_1 (y - x)\right) - \beta_2 V\left(x + \Pi_2 (y - x)\right) - \beta_{1,2} V\left(x + \Pi_{1,2} (y - x)\right). \end{aligned}$$

In parallel to Theorem 1, we have the following theorem for the index-m case. Its proof is similar to the proof of Theorem 1 but technically lengthier and thus is skipped.

Theorem 5. *Assume that $V(x) \in \mathcal{C}^4(\mathbb{R}^d; \mathbb{R})$. For each x, let $v_1(x), \ldots, v_m(x)$ be m normalized eigenvectors corresponding to the smallest eigenvalues of the Hessian matrix $H(x) = \nabla^2 V(x)$, i.e.,*

$$[v_1(x), \ldots, v_m(x)] = \operatorname*{argmin}_{U = [u_1, \ldots, u_m],\, U^{\mathsf{T}} U = I} \operatorname{trace}\, U^{\mathsf{T}} \nabla^2 V(x) U.$$

The function $L(y; x, \alpha, \beta)$ of the variable y is defined as in (20) and it is assumed that

$$\sum_{s \in S} (\alpha_s + \beta_s) > 1,$$

Suppose that x^* is an index-m saddle point of the function $V(x)$. Then the following statements are true.

(i) x^* is a local minimizer of $L(y; x^*, \alpha, \beta)$.

(ii) There exists a neighborhood $\mathcal{U}$ of x^* such that for any $x \in \mathcal{U}$, $L(y; x, \alpha, \beta)$ has a unique minimum in $\mathcal{U}$. We define $\Phi(x)$ to be this minimizer for the given x.

(iii) The mapping Φ has only one unique fixed point x^* in $\mathcal{U}$.

(iv) The mapping Φ is differential in $\mathcal{U}$. The Jacobi matrix of Φ vanishes at x^*, i.e.,

$$\Phi_x(x^*) = 0.$$

As a consequence of the above theorem, the following iterative scheme

$$\begin{cases} x^{(k+1)} = \underset{y}{\operatorname{argmin}}\ L(y; x^{(k)}, \alpha, \beta) \\ [v_1^{(k+1)}, \ldots, v_m^{(k+1)}] = \underset{U=[u_1,\ldots,u_m],\, U^\mathsf{T}U=I}{\operatorname{argmin}} \operatorname{trace}\, U^\mathsf{T} \nabla^2 V(x^{(k)}) U \end{cases}$$

converges to the index-m saddle point x^* quadratically if the starting point $x^{(0)}$ is close enough to x^*.

6. Examples

6.1. **A simple two dimensional example.** Firstly, we review a two dimensional example in [11].

$$V(x, y) = \frac{1}{4}(x^2 - 1)^2 + \frac{1}{2}\mu y^2$$

where μ is a positive parameter. For this system, $x_\pm = (\pm 1, 0)$ are two local minima and $(0, 0)$ is the index-1 saddle point. The eigenvalues and eigenvectors of the Hessian matrix at a point (x, y) are

$$\begin{aligned} &\lambda_1 = 3x^2 - 1 \ \text{ and } \ v_1 = (1, 0), \\ &\lambda_2 = \mu \ \text{ and } \ v_2 = (0, 1). \end{aligned}$$

Note that when $|x| \le \sqrt{\frac{1+\mu}{3}}$, $\lambda_1 \le 0 < \lambda_2$. The eigenvector corresponding to the smallest eigenvalue is v_1 if $|x| < \sqrt{\frac{1+\mu}{3}}$ and becomes v_2 if $|x| > \sqrt{\frac{1+\mu}{3}}$.

Suppose that at iteration k, the position is (x_k, y_k). Then, the modified objective functions $V + W_1$ and $V + W_2$ in the iterative minimization method is defined as follows

$$\begin{cases} V + W_1^{(k)} = -\frac{1}{4}(x^2 - 1)^2 + \frac{1}{2}\mu y^2 + \frac{1}{2}(x_k^2 - 1)^2 & \text{if } |x| < \sqrt{\frac{1+\mu}{3}}, \\ V + W_1^{(k)} = \frac{1}{4}(x^2 - 1)^2 - \frac{1}{2}\mu y^2 + \mu y_k^2 & \text{if } |x| > \sqrt{\frac{1+\mu}{3}}. \end{cases}$$

$$\begin{cases} V + W_2^{(k)} = -\frac{1}{4}(x^2 - 1)^2 + \frac{1}{2}\mu y^2 - \mu y_k^2 & \text{if } |x| \le \sqrt{\frac{1+\mu}{3}}, \\ V + W_2^{(k)} = \frac{1}{4}(x^2 - 1)^2 - \frac{1}{2}\mu y^2 - \frac{1}{2}(x_k^2 - 1)^2 & \text{if } |x| > \sqrt{\frac{1+\mu}{3}}. \end{cases}$$

These are piecewise continuous function and the difference of W_1 and W_2 is only a constant. In the domain where $|x| < \min\left(1, \sqrt{\frac{1+\mu}{3}}\right)$, the original saddle $(0, 0)$ is the unique interior minimal point. Outside of this domain, the modified function $V + W_1$ or $V + W_2$ has no lower bound. So, the iterative minimizing method works only when the initial guess satisfies $|x| < \sqrt{\frac{1+\mu}{3}}$.

6.2. **The three-hole example.** In the second example, we study a two dimensional energy function in [22, 19] where there are three local minima. The formula of this energy function is

$$V(x,y) = 3e^{-x^2-(y-\frac{1}{3})^2} - 3e^{-x^2-(y-\frac{5}{3})^2} - 5e^{(x-1)^2-y^2} - 5e^{(x+1)^2-y^2} + 0.2x^4 + 0.2\left(y-\frac{1}{3}\right)^4.$$

Refer to Figure 1 for the contour plot.

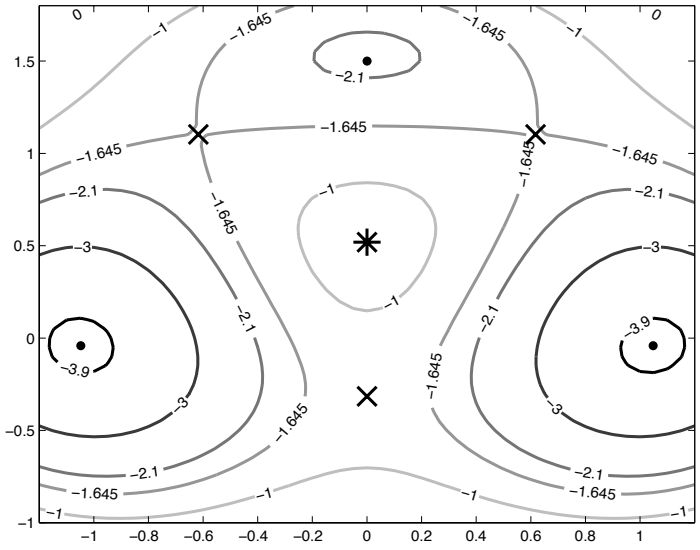

FIGURE 1. Three-hole potential: three minima (black dots) approximately at $(\pm 1, 0)$ and $(0, 1.5)$, a maximum ("$*$") at $(0, 0.5)$ and three saddle points ("$\times$") at $(0, -0.31582)$ and $(\pm 0.61727, 1.10273)$.

Let SP1 $= (0, -0.31582)$ and SP2 $= (-0.61727, 1.10273)$ be the two saddles of interests. We first demonstrate the quadratic convergence when the initial guess is near the saddle points. Table 1 shows the errors at each iterations, from which it is observed that the iterative scheme has the quadratic convergence rate.

Iter	$(2,0)$	$(0,2)$	$(1,1)$	$(2,0)$	$(0,2)$	$(1,1)$
1	5.042e-002	2.979e-002	2.924e-002	1.672e-002	3.024e-002	4.342e-002
2	1.376e-005	5.470e-004	1.671e-004	9.327e-006	3.445e-004	3.194e-004
3	7.245e-011	2.573e-008	2.434e-008	2.527e-011	1.116e-008	1.233e-008
4	5.023e-016	5.551e-016	3.951e-016	2.482e-016	3.886e-016	4.965e-016

TABLE 1. Errors of 6 runs with random initial guesses circled at the target saddle point with 0.2 radius. Different values of (α, β) for the modified objective functions in subproblem are shown in the brackets.The left 3 runs converge to SP1 and the right 3 runs converge to SP2.

Iter	$(2,0)$	$(0,2)$	$(1,1)$	$(2,0)$	$(0,2)$	$(1,1)$
1	8.434e-001	8.568e-001	8.496e-001	1.160e+000	1.170e+000	1.262e+000
2	6.891e-001	7.026e-001	6.954e-001	9.922e-001	9.970e-001	1.077e+000
3	5.731e-001	5.858e-001	5.790e-001	8.512e-001	8.537e-001	9.464e-001
4	5.216e-001	5.317e-001	5.263e-001	6.983e-001	6.939e-001	8.020e-001
5	3.862e-001	3.848e-001	3.841e-001	5.273e-001	5.028e-001	6.397e-001
6	1.776e-001	1.740e-001	1.742e-001	3.391e-001	3.030e-001	4.542e-001
7	1.983e-002	4.266e-002	1.987e-002	1.511e-001	1.291e-001	2.569e-001
8	7.314e-007	3.343e-004	2.834e-004	2.975e-002	1.207e-002	8.031e-002
9	3.756e-012	9.654e-009	4.088e-008	2.093e-006	2.879e-005	3.919e-003
10		6.810e-016	7.773e-015	1.734e-015	1.912e-011	7.345e-006
11					3.140e-016	2.745e-011

TABLE 2. Errors of 6 random runs with initial guesses circled at a local minimum $(-1,0)$ with 0.1 radius. The three runs on the left columns converge to SP1 and the other three runs on the right columns converge to SP2 respectively.

Iter	$(2,0)$	$(0,2)$	$(2,0)$	$(0,2)$
1	4.476e-02	2.723e-02	5.096e-02	1.877e-02
2	1.262e-04	3.256e-04	7.756e-05	8.386e-04
3	2.863e-08	6.047e-06	1.270e-09	4.176e-05
4	5.317e-13	3.316e-10	7.830e-13	1.8827e-09
5		7.325e-13		4.3853e-11

TABLE 3. Errors of 4 runs with random initial guesses circled at the target saddle points with 0.2 radius. Use three-step nonlinear CG method to solve the subproblem of minimization inexactly. The left 2 runs converge to SP1 and the right 2 runs converge to SP2 respectively.

If the initial guess is close to the local minima of V, then the Hessian of V at the initial point is positive-definite, while the modified objective function has one negative eigenvalue and has no lower bound. As discussed in §3.3, we set a maximum step size 0.25 both in x and y direction at each iteration to maintain the stability at this initial stage. Equivalently, it is to solve the subproblem in the square box of size 0.25. Table 2 shows the result for initial points which are 0.1 away from $(-1,0)$, one of the two deep minima. Some runs converge to SP2 and others converge to SP1. It is observed that at the first few steps, the decreasing of the errors is slow but when it approaches to the saddle, the smallest eigenvalue of the Hessian becomes negative, and it follows that the iterative minimization method starts to show quadratic convergence.

We also test the effects of the inexact solution of the subproblem. In solving the subproblem by the conjugate gradient method, we only perform three steps of conjugate gradient search. The initial guesses are chosen on the circle centered at the saddle points with 0.2 radius. The results are shown in Table 3 with two different parameter sets ($\alpha = 2, \beta = 0$ and $\alpha = 0, \beta = 2$). In comparison to the case of exact solution for subproblem in Table 1, the efficiency of the algorithm is not affected much and the local convergence rate is still quite close to the second order.

In the end, for this 2-D example, we plot the domain of attraction for our algorithm to compare with the performance of the Newton method. Note that our purpose here is to look for index-1 saddle points. We choose initial guesses from 50×50 grid points uniformly in the rectangular region $[-1.5, 1.5] \times [-1.5, 2.0]$. These points are labelled in Figure 2 by three different marks in three colours, according to which saddle point (shown in cross sign) they converge to. The grid point is left blank in case of no convergence to any saddle. The figure demonstrates that our IMF scheme has a larger (and continuous) domain of attraction for each saddle point.

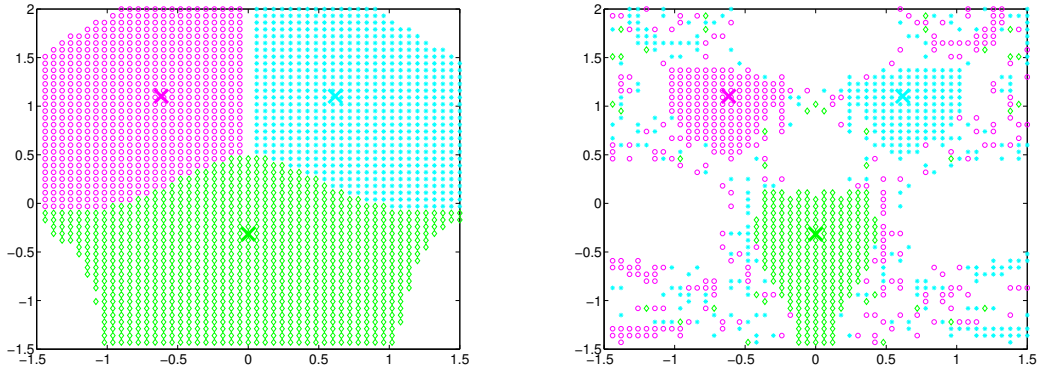

(A) IMF (B) Newton

FIGURE 2. Comparison of domain of attractions for saddle search problem in our scheme and Newton scheme.

6.3. **A quadratic function on the sphere S^2.** We illustrate the proposal in Section 4 for the constrained problem by considering a simple example of $\mathcal{M} = S^2$ embedded in $\mathbb{R}^3$ on which a quadratic energy function $V(x_1, x_2, x_3) = x_1^2 + 2x_2^2 + 3x_3^2$ is defined. The constraint is that $x_1^2 + x_2^2 + x_3^2 = 1$. It is easy to verify that saddle points $(0, \pm 1, 0)$, minimizers $(\pm 1, 0, 0)$ and maximizers $(0, 0, \pm 1)$ of V are generated due to this constraint.

As mentioned in Section 4, for a given $x \in S^2$ and $v \in \mathcal{T}_x(S^2)$, the projection of a point y on S^2 is associated with a geodesic curve $\xi(s)$. Here the geodesic ξ is simply the great circle passing the point x along the direction v. Thus ξ can be written in the parameterized form $\xi(\theta) = x\cos\theta + v\sin\theta$. It follows that the geodesic distance $\text{dist}(\xi(\theta), y) = \arccos\langle\xi(\theta), y\rangle$ achieves the minimum at $\theta = \theta_y$, where θ_y is equal to $\arctan\frac{\langle v,y\rangle}{\langle x,y\rangle}$ or $\arctan\frac{\langle v,y\rangle}{\langle x,y\rangle} + \pi$ depending on which value gives smaller distance. Then the projection point of y is $x\cos\theta_y + v\sin\theta_y$. So we have $W_2(y) = -2V(x\cos\theta_y + v\sin\theta_y)$ for this S^2 example.

Next we also derive W_1 expression for this S^2 case. Since the tangent space $\mathcal{T}_x(S^2)$ is two dimensional, the orthogonal complement of v in this space is spanned by just a single vector, denoted as $\tilde{v}$. It follows then that $W_1(y) = -2V(y) + 2V(x\cos\tilde{\theta}_y + v\sin\tilde{\theta}_y)$ where $\tilde{\theta}_y$ is defined likely as θ_y by substituting v by $\tilde{v}$.

The numerical results based on the construction of the above W_1 and W_2 are presented in Table 4. The initial guess is 0.1 distant to the minimum point $(1, 0, 0)$. The numerical

data of the errors between the solution and the true saddle point in this table again confirm the quadratic convergence rate. We remark that it is important to use the projection associated with the geodesic curve in the construction of W_1 and W_2. One alternative idea might use the projection in the Euclidean space $\mathbb{R}^3$ as if no constraints, then pull-back to S^2. For instance, one may use the following $W_2(y) = -2V\left(R_x(v^{\mathsf{T}}(y-x)v)\right)$, where $R_x(u) = \frac{x+u}{\|x+u\|}$ is a retraction mapping the tangent space $\mathcal{T}_x$ to the sphere S^2. However, our numerical result for the same example here shows that this choice gives only a linear convergence rate. The missing curvature information of the manifold in this naive orthogonal projection approach seems to be the reason of lowering the convergence order.

Iter	1	2	3	4	5
$V + W_1$	1.3900e+00	2.3217e-01	1.4234e-03	2.0994e-08	1.7684e-15
$V + W_2$	1.2902e+00	5.6506e-01	6.5923e-02	8.7484e-06	1.2433e-16

TABLE 4. Errors of S^2 example

6.4. **An atomic model system.** This is an application of our method to the celebrated test problem of a 7 atoms island on the (111) surface of an FCC metal [12]. In this example the structure has a 6-layer slab, each of which contains 56 atoms, and 7 atoms at the top of the slabs. The bottom three layers in the slab are frozen. There are $56 \times 3 + 7 = 175$ atoms are free to move. All the atoms in this simulation are identical.

The interaction between the atoms is the simple pairwise additive Morse potential

$$V(R) = A[e^{-2a(R-R_0)} - 2e^{-a(R-R_0)}]$$

with parameters chosen to reproduce diffusion barriers on Pt surfaces ($A = 0.7102$eV, $a = 1.6047\mathring{A}^{-1}$, $R_0 = 2.8970\mathring{A}$). This potential is cut and shifted by V(R_C) where $R_C = 9.5\mathring{A}$ is the cut-off distance. The minimum energy lattice constant $2.74412\mathring{A}$ is used.

We show two local minima in Figure 3 as well as two saddle points. All saddle points lead from the close packed heptamer (shown in red) to some adjacent state. We applied our iterative minimization method to this large-scale system. The initial guess of position is chosen near the minima. And the initial direction is randomly selected. The eigenvector corresponding to the minimum eigenvalue is solved by an efficient LOR method proposed in [17]. The maximum step size in the subproblem for the position is set as 0.2. In this implementation, we used nonlinear conjugate-gradient method with the tolerance set to 10^{-16} so that the subproblem is solved accurately enough. The accuracy of the each entry in the force at the saddle points is between 10^{-10} and 10^{-11}. The error is defined as the Euclidean distance from the current position to the saddle.

The numerical results are presented in Table 5. Since our initial guess is very close to the local minimum, it is not surprising that the first several iteration steps have a slow decay of the errors since the effect of following the eigenvector of the smallest eigenvalue has not kicked in. The fast convergence rate is observed as expected in the second part. In this example, the exact solver for each subproblem was used in Table 5, thus the computational overhead is large, compared with other algorithms requiring no subproblems to solve. We also introduced a simple inexact solver by limiting only two iterations of CG for subproblem. The resulting convergence rate deteriorates due

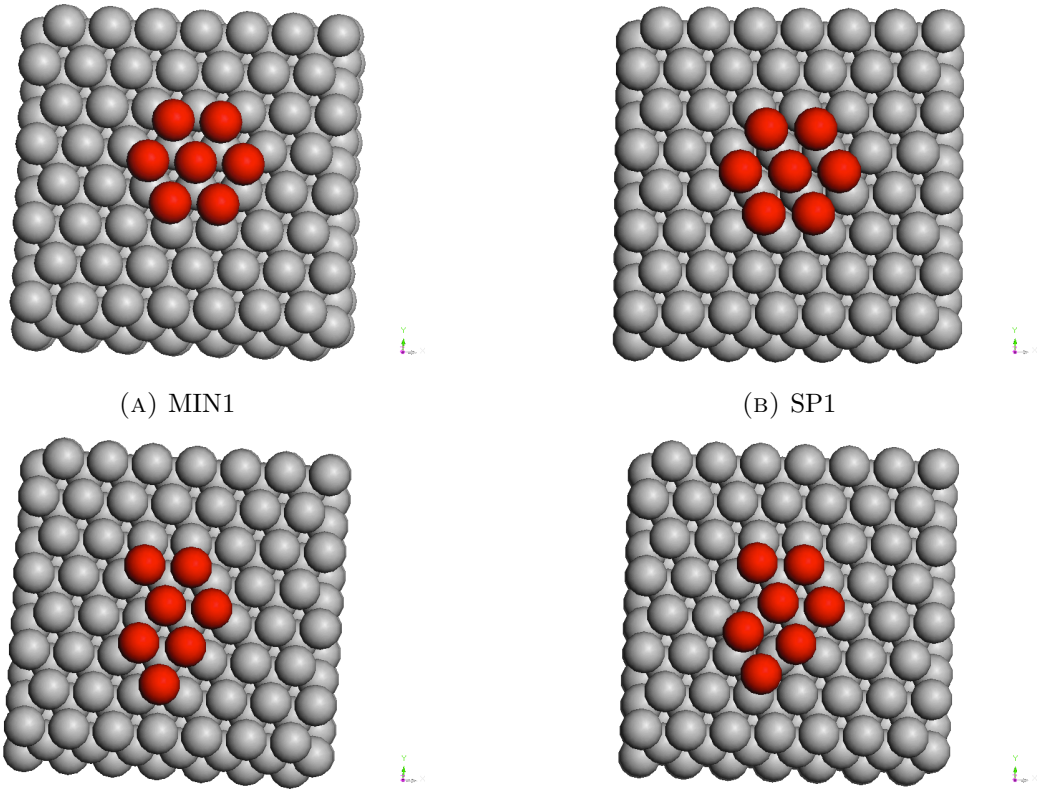

(A) MIN1 (B) SP1

(C) MIN2 (D) SP2

FIGURE 3. The 7-atom island model. Two local minima and two saddle points are shown and denoted as MIN1, SP1, MIN2, SP2, respectively.

to inexact solver and linear convergence is observed. The right balance between the fast convergence rate and the large computational overhead requires a careful design of the tolerance in the inexact solver.

7. Concluding remarks

This paper presents a new formulation of iterative minimization to the saddle search problem. In this formulation, the problem is solved by iteratively solving a sequence of minimization subproblems. At each iteration, the rotation step of determining the softest eigenvector v is followed by a nonlinear optimization for the subproblem to update the x variable. We have proved the local quadratic convergence rate of the new scheme. This new scheme is closely connected to the gentlest ascent dynamics (GAD) and other "eigenvector-following" algorithms such as the dimer method. However, our subproblem is not limited only on the direction of v, but includes the information of the original energy function in all directions to update the x variable in $\mathbb{R}^d$. The quadratic convergence rate theoretically established here is promising for further numerical improvement in practice and indicates that this could be the best rate for "eigenvector-following"-class algorithms. In a forthcoming paper, we shall address the implementation of efficient algorithms based on this formulation. We are also interested in the saddle points of the free

Iter	$V+W_1$	$V+W_2$	$\frac{2V+W_1+W_2}{2}$	$V+W_1$	$V+W_2$	$\frac{2V+W_1+W_2}{2}$
1	2.014e+000	1.832e+000	1.803e+000	1.633e+000	1.695e+000	1.521e+000
2	1.837e+000	1.695e+000	1.760e+000	1.599e+000	1.575e+000	1.488e+000
3	1.729e+000	1.575e+000	1.693e+000	1.535e+000	1.314e+000	1.433e+000
4	1.621e+000	1.315e+000	1.603e+000	1.446e+000	8.668e-001	1.336e+000
5	1.454e+000	8.668e-001	1.536e+000	1.312e+000	4.061e-001	1.167e+000
6	1.345e+000	4.496e-001	1.420e+000	1.114e+000	2.897e-001	9.808e-001
7	1.129e+000	1.605e-001	1.205e+000	9.250e-001	1.875e-001	7.974e-001
8	6.903e-001	3.335e-001	1.009e+000	7.405e-001	1.072e-001	6.113e-001
9	3.189e-001	8.653e-002	8.068e-001	5.605e-001	5.076e-002	4.407e-001
10	2.552e-001	9.040e-003	6.063e-001	3.855e-001	5.951e-003	2.679e-001
11	1.297e-001	3.398e-005	4.252e-001	2.016e-001	8.782e-006	1.058e-001
12	1.170e-002	6.333e-008	2.526e-001	3.005e-002	1.132e-007	1.903e-002
13	1.536e-004	2.641e-010	1.011e-001	5.290e-004	1.579e-009	5.277e-004
14	9.017e-008		1.141e-002	1.367e-008		8.758e-007
15	3.907e-010		1.487e-004	1.135e-009		3.347e-008
16			7.792e-008			

TABLE 5. Errors of 6 runs with random initial guesses near the local minima as well as with different additional potentials. The left 3 runs start from the initial guesses near MIN1 and converge to SP1. The right 3 runs start from the initial guesses near MIN2 and converge to SP2, respectively.

energy landscape in collective variables, where the free energy function V is not known, but the force, the Hessian and even the third order perturbation can be simultaneously computed from one single, but expensive, run of constrained molecular dynamics [18].

ACKNOWLEDGMENT

The work of W. Gao is supported by the National Natural Science Foundation of China under grants 91330202, Shanghai Science and Technology Development Funds 13dz2260200, 13511504300. X. Zhou acknowledges the financial support of CityU Start-Up Grant (7200301) and Hong Kong Early Career Schemes (109113). The authors would like to thank the anonymous referees for valuable suggestions.

REFERENCES

[1] P.-A. Absil, R. Mahony, and R. Sepulchre. *Optimization Algorithms on Matrix Manifolds*. Princeton University Press, 2007.

[2] J. F. Bonnas and A. Shapiro. Optimization problems with perturbations: a guided tour. *SIAM Rev.*, 40:228–264, 1998.

[3] C. A. Botsaris. Constrained optimization along geodesics. *J. Math. Anal. Appl.*, 79(2):295–306, 1981.

[4] E. Cancès, F. Legoll, M.-C. Marinica, K. Minoukadeh, and F. Willaime. Some improvements of the activation-relaxation technique method for finding transition pathways on potential energy surfaces. *J. Chem. Phys.*, 130:114711, 2009.

[5] A. Cauchy. Méthode générale pour la ésolution des systéms d'equations simultanées. *Comp. Rend. Sci. Paris*, 25:46–89, 1847.

[6] C. J. Cerjan and W. H. Miller. On finding transition states. *J. Chem. Phys.*, 75(6):2800–2806, 1981.

[7] G. M. Crippen and H. A. Scheraga. Minimization of polypeptide energy : XI. the method of gentlest ascent. *Arch. Biochem. Biophys.*, 144(2):462–466, 1971.

[8] Qiang Du and Lei Zhang. A constrained string method and its numerical analysis. *Commun. Math. Sci.*, 7:1039–1051, 2009.

[9] W. E, W. Ren, and E. Vanden-Eijnden. String method for the study of rare events. *Phys. Rev. B*, 66:052301, 2002.

[10] W. E, W. Ren, and E. Vanden-Eijnden. Simplified and improved string method for computing the minimum energy paths in barrier-crossing events. *J. Chem. Phys.*, 126:164103, 2007.

[11] W. E and X. Zhou. The gentlest ascent dynamics. *Nonlinearity*, 24(6):1831, 2011.

[12] G. Henkelman, G. Jóhannesson, and H. Jónsson. Methods for finding saddle points and minimum energy paths. In S. D. Schwartz, editor, *Progress on Theoretical Chemistry and Physics*, pages 269–300. Kluwer Academic Publishers, 2000.

[13] G. Henkelman and H. Jónsson. A dimer method for finding saddle points on high dimensional potential surfaces using only first derivatives. *J. Chem. Phys.*, 111(15):7010–7022, 1999.

[14] A. Henry, A. T.Bell, and F. J.Keil. Efficient methods for finding transition states in chemical reactions: Comparison of improved dimer method and partitioned rational function optimization method. *J. Chem. Phys.*, 123:224101, 2005.

[15] H. Jònsson, G. Mills, and K. W. Jacobsen. Nudged elasic band method for finding minimum energy paths of transitions. In B. J. Berne, G. Ciccotti, and D. F. Coker, editors, *Classical and Quantum Dynamics in Condensed Phase Simulations*, page 385, New Jersey, 1998. LERICI, Villa Marigola,Proceedings of the International School of Physics, World Scientific.

[16] J. Kästner and P. Sherwood. Superlinearly converging dimer method for transition state search. *J. Chem. Phys.*, 128:014106, 2008.

[17] J. Leng, W. Gao, C. Shang, and Z.-P. Liu. Efficient softest mode finding in transition states calculations. *J. Chem. Phys.*, 138(9):094110, 2013.

[18] L. Maragliano, A. Fischer, E. Vanden-Eijnden, and G. Ciccotti. String method in collective variables: Minimum free energy paths and isocommittor surfaces. *J. Chem. Phys.*, 125(2):024106, 2006.

[19] P. Metzner, C. Schüttle, and E. Vanden-Eijnden. Illustration of transition path theory on a collection of simple examples. *J. Chem. Phys.*, 125(8):084110, 2006.

[20] N. Mousseau and G.T. Barkema. Traveling through potential energy surfaces of disordered materials: the activation-relaxation technique. *Phys. Rev. E*, 57:2419, 1998.

[21] J. Nocedal. *Numerical Optimization*. Springer Series in Operations Research. Springer-Verlag, 1999.

[22] S. Park, M. K. Sener, D. Lu, and K. Schulten. Reaction paths based on mean first-passage times. *J. Chem. Phys.*, 119(3):1313–1319, 2003.

[23] W. Ren and E. Vanden-Eijnden. A climbing string method for saddle point search. *J. Chem. Phys.*, 138:134105, 2013.

[24] A. Samanta and W. E. Atomistic simulations of rare events using gentlest ascent dynamics. *J. Chem. Phys.*, 136:124104, 2012.

[25] D. J. Wales. *Energy Landscapes with Application to Clusters, Biomolecules and Glasses*. Cambridge University Press, 2003.

[26] J. Zhang and Q. Du. Constrained shrinking dimer dynamics for saddle point search with constraints. *J. Comput. Phys.*, 231:4745–4758, 2012.

[27] J. Zhang and Q. Du. Shrinking dimer dynamics and its applications to saddle point search. *SIAM J. Numer. Anal.*, 50:1899–1921, 2012.